Chiang Mai J. Sci. 2014; 41(5.2) : 1220-1229
http://epg.science.cmu.ac.th/ejournal/
Contributed Paper

Effects of Silicon-Bridge and π-Ligands on the Electronic Structures and Related Properties of Dimethyl Zirconocene Polymerization Catalysts: A Comparative Theoretical Study

Jitrayut Jitonnom*[a] and Wijitra Meelua [a,b]

[a] Division of Chemistry, School of Science and [b] Demonstration School, University of Phayao, Phayao 56000, Thailand.

*Author for correspondence; e-mail: jitrayut.018@gmail.com

Received: 2 June 2013
Accepted: 27 July 2013

ABSTRACT

Group 4 metallocene has gained more attention recently as a potential catalyst for ring-opening polymerization of lactones. Introduction of a silicon-bridge and/or modifications of biscyclopentadiene (Cp_2) ligand with different π-ligands such as bisindene (Ind_2), mixed indene/cyclopentadiene (CpInd) or mixed uorene/cyclopentadiene (CpFlu) have been found to significantly help improve catalyst activities, polymer yields and molecular weight. In order to relate the silicon bridge (B) and π-ligand (L) effects with the catalyst activities, molecular structures and properties of those bridged dimethylzirconocene complexes as well as their insertion behaviors with ε-caprolactone were investigated by using the density functional theory method. Calculations showed that different π-ligands had a profound effect on the electronic geometries and related properties of the title complexes. All bridged catalysts were geometric constraints compared to the unbridged catalysts. The HOMO-LUMO gap and dipole moments were decreased as the large π-ligands were introduced (Cp_2 > CpInd > Ind_2 > CpFlu). Only Si and Zr atoms were observed to carry a positive charge with Si having the most. For the monomer-inserted complexes, most catalyst structures shared the same orientation of ε-caprolactone with its ester group pointing away from a methyl group of Zr atom, except the catalyst with Ind_2 ligand due to steric hindrance. A planar conformation of the monomer was observed in all catalysts and, hence, is required for each insertion. The data provide a structural basis for both inactivated and activated bridged-dimethylzirconocene complex catalysts with different π-ligands, which will be helpful for further studies on the lactone polymerization initiated by group 4 metallocene.

Keywords: silicon-bridge, zirconium, metallocene, density functional theory

1. INTRODUCTION

Ring-opening polymerization (ROP) of lactones represents a growing field of polymer research because the produced polyesters are biodegradable and biocompatible materials potentially used for biomedical and pharmaceutical applications as well as

environmentally friendly materials [1-3]. Several metal complexes have been well established for the ROP of lactones, such as alkoxides of Li [4], Al [5], Sn [6], Zn [7], Ln [8] and Ti [9]. Apart from these metal alkoxides, group 4 metallocenes have drawn increased attention, as an interesting group of transition metal complexes potentially applied for the ROP of lactones.

Previous studies have reported the use of dimethylzirconocene complexes, as pre-catalyst for the ROP of lactones with various substituted cyclopentadienyl (Cp), indenyl (Ind) and uorenyl (Flu) ligands and a bridge in the catalytic systems. Hayakawa et al. [10] was one of the first to report the ROP of lactones initiated by zirconocene-borate complex catalysts, which was found to proceed via cationic mechanism (Figure 1). Their catalytic system used is based on bis(cyclopentadiene), Cp_2ZrMe_2 and $CpCp^*ZrMe_2$ (Cp*: pentamethyl cyclopentadiene) with high molecular weights and low polydispersities of polylactone obtained. Kostakis et al. [11] reported the polymerization of ε-CL and δ-VL using various catalytic systems consisting of a combination of three C_{2v} zirconocene complexes and three borate cocatalysts. They introduced the bis(indene) ligand, Ind_2ZrMe_2, and also the Cp_2ZrMe_2, $(tBuCp)_2ZrMe_2$ in the zirconocene catalytic systems to initiate the polymerizations, producing polymers with relatively high molecular weights and narrow molecular weight distributions. Recently, Villaseñor et al. [12] have first introduced the *ansa*-zirconocene complex with silicon methyl (Me_2Si) as a bridge for the ROP of ε-CL. They successfully synthesized mixed indenyl/cyclopentadienyl zirconocene systems, $CpIndZrMe_2$, with and without the silicon bridge and used them in the polymerizations, yielding the resulting polymer with impressive quantitative outcome without cocatalyst (medium molecular weight polymers with moderate to broad polydispersities). Based on those studies, modifications of the π-ligands and the bridge in the catalyst are key factors to improve the catalytic activity, and thus guiding a development of group 4 metallocene complexes for the use as potential catalysts of the ROP of lactones. This has inspired us for a requirement of fundamental understanding of electronic effect of the π-ligands and the bridge on the efficiency of *ansa*-zirconocene catalysts in the ROP of ε-CL.

In this work, the electronic structures and related properties of four *ansa*-dimethylzirconocene complexes (**I-IV**) bearing Cp, Ind or Flu ligands (see Figure 2) were comparatively investigated by means of density functional theory. We analyzed the electronic geometries of the catalysts when the *ansa*-bridge and the ε-ligands are introduced to understand their structural basis. We continued analyzing the regioselectivity of the ε-CL monomer to the four catalysts during the monomer-insertion step by finding the most stable structure of the monomer-inserted complexes for each catalyst. To the best of our knowledge, the comparisons of the electronic structures and properties of catalysts **I-IV** have not been investigated theoretically.

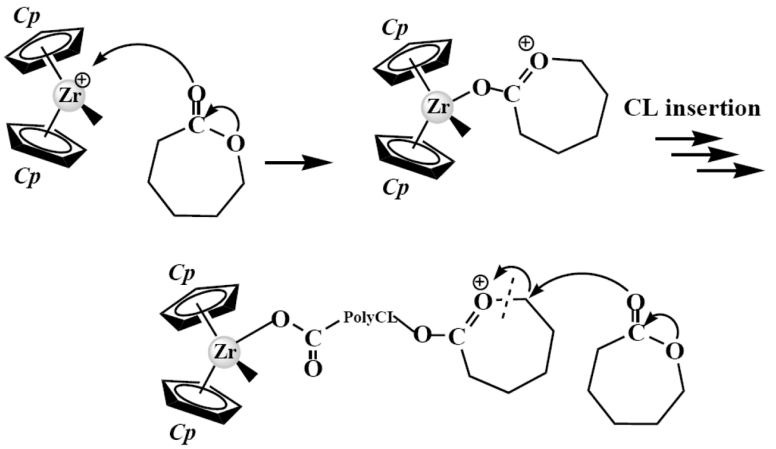

Figure 1. Cationic ROP mechanism of lactones initiated by dimethylzirconocene catalyst, Cp_2ZrMe_2.

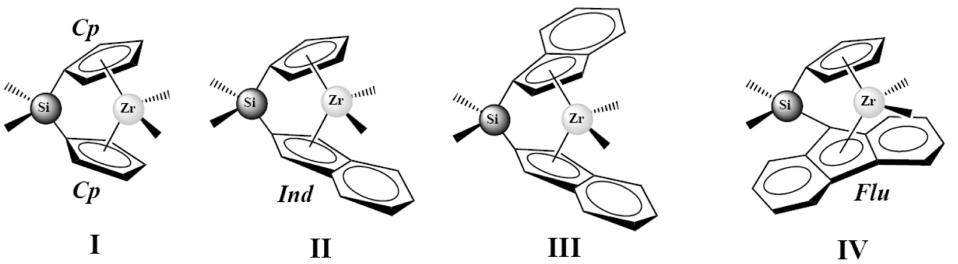

Figure 2. Generic structure of silicon-bridged dimethylzirconocene complex with different π-ligands.

2. MATERIAL AND METHODS

Geometries at the standard state (298 K and 1 atm) of all title complexes were optimized using Hartree Fock (HF) and Density Functional Theory (DFT) at the B3LYP level with the Gaussian09 program [13]. This popular and computationally cheap method predicted reliable geometries and quantum chemical results. We used a double-ζ basis set (6-31G*) for all non-metal atoms and the effective core potential double-ζ basis set (LANL2DZ) [14] for zirconium and silicon atoms. This mixed basis set was created through the use of the GEN keyword in Gaussian09. Both of these basis sets have been widely used along with DFT methods for the study of transition metal containing systems [14, 15]. Note that the chosen DFT methods were used only for describing the gas-phase structures of catalysts, which does not account for the dynamics of monomer and/or catalyst in solution.

3. RESULTS AND DISCUSSION

3.1 Comparison of the Computed Structure with the X-ray Structure

Although the popular DFT method is widely used for locating the stable geometries of transition metal complexes [15], it is important to compare the DFT optimized structure of the investigated system with the available crystal structure in order to test the reliability of the method. To this end, catalyst **II** was chosen as a test model to compute its geometry at HF/LANL2DZ and B3LYP/LANL2DZ methods. The results are summarized in Table 1, along

with the experimental observation from the literature [12]. In general, the optimized geometry of catalyst **II** from the B3LYP/LANL2DZ method is more reasonably agreement with the X-ray crystal structure than that from the HF/LANL2DZ method, as evidenced by a relatively low mean absolute error (0.48 for B3LYP/LANL2DZ and 0.64 for HF LANL2DZ). The HF method gave an overestimation for most bond lengths compared to those structural parameters from the B3LYP method, for example, the distances of Zr-Cen1 and Zr-Cen2 bonds are calculated at 2.326/2.359 Å (HF) and 2.289 2.320 Å (B3LYP), higher than the X-ray observation (2.222/2.264 Å), respectively. The Cen1-Zr-Cen2 angles are calculated at 124.8° (HF) and 126.3° (B3LYP), which is close to the X-ray structure (128.1°). This result represents a case where the exchange and correlation functional is necessary, supporting the benefit of the B3LYP method over the HF method for studying the transition metal complex.

Table 1. Experimental and calculated bond lengths and bond angles for catalyst **II.**

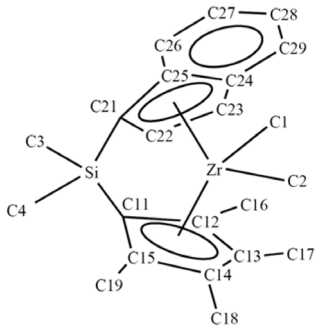

		Calculation			
Bond length, angle	X-ray[a]	HF	error	B3LYP	error
Zr–C1	2.267	2.285	0.018	2.271	0.004
Zr–C2	2.271	2.295	0.024	2.282	0.011
Zr–C21	2.485	2.552	0.067	2.536	0.051
Zr–C22	2.500	2.561	0.061	2.537	0.037
Zr–C23	2.600	2.685	0.085	2.661	0.061
Zr–C24	2.670	2.79	0.120	2.777	0.107
Zr–C25	2.580	2.703	0.123	2.686	0.106
Si–C3	1.860	1.895	0.035	1.897	0.037
Si–C4	1.866	1.899	0.033	1.901	0.035
Si–C11	1.880	1.911	0.031	1.908	0.028
Si–C21	1.867	1.893	0.026	1.894	0.027
Zr-Cen1	2.222	2.326	0.104	2.289	0.067
Zr-Cen2	2.264	2.359	0.095	2.320	0.056
av Zr–C(Cen1)[b]	2.531	2.599	0.068	2.588	0.057
av Zr–C(Cen2)[b]	2.567	2.658	0.091	2.639	0.072
C1–Zr–C2	96.4	96.0	0.4	98.5	2.1
C3–Si–C4	107.4	104.9	2.5	105.5	1.9
C11–Si–C21	97.1	96.6	0.5	96.6	0.5
Cen1–C11–Si	160.6	163.9	3.3	162.5	1.9
Cen2–C21–Si	161.5	164.0	2.5	162.7	1.2
Cen1–Zr–Cen2	128.1	124.8	3.3	126.3	1.8
Mean absolute error			0.64		0.48

[a] Taken from Ref [11]. [b] Refers to the average bond length between Zr and the carbon atoms of the C5 ring of the corresponding cyclopentadienyl moiety. Cen1 and Cen2 are the centroids of C11–C15 and C21–C25, respectively. For clarity, the figure representing a chemical structure of catalyst **II** is included without the hydrogen atoms.

3.2 The Bridging Effect on the Electronic Geometries of Catalysts I-IV

The optimized structures of catalysts **I-IV** calculated at the B3LYP/LANL2DZ level of theory are illustrated in Figure 3 and their corresponding geometric parameters are listed in Table 2. It appears that silicon bridge (Me_2Si) has a significant effect to the catalyst structure compared to the unbridge one: it reduces the angle (α) formed between the metal and the two π-ligands and increases the angle (β) formed between the plane of π-ligands: for catalyst **I** the α and β values are calculated at 124.9° and 59.9°, respectively, for the bridge but are 133.8° and 46.1° for the unbridge. Similar observation was also found for other catalysts (see Table 2). More compact structures were observed for all bridging catalysts, as evidenced by the decreased distances between two centroids of π-ligands (Cen-Cen) and between the metal and the centroid (M-Cen) shown in Table 2. With a constrained geometry in the catalysts, the metal must arrange itself to fit with the packed structure, leading to increase the D distance in all four catalysts, especially in the catalyst **III** (with the maximum extent of D = ~0.4 Å). This metal extension may facilitate the cocatalyst activation and/or monomer insertion.

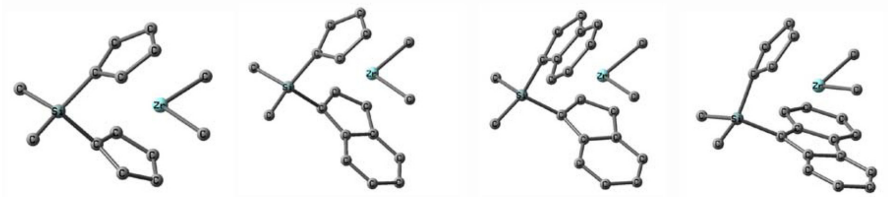

Figure 3. Optimized structures of catalysts **I-IV** calculated at the B3LYP/LANL2DZ level of theory.

Table 2. Geometric parameters for the optimized structures of catalysts **I-IV** calculated at the B3LYP/LANL2DZ level of theory. The geometric structures of the unbridged silicon of catalysts **I-IV** are also indicated in parenthesis.

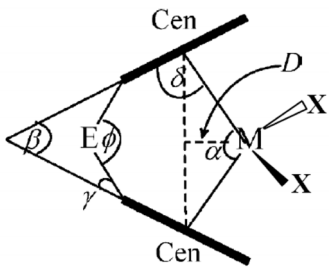

Catalyst	Φ	Cen-Cen (Å)	D (Å)	α (°)	β (°)	γ (°)	δ (°)	M-Cen (Å)	M-X (Å)	X-M-X (°)	E-M (Å)
I	81.98	4.05	1.05	124.9	59.9	17.9	87.5	2.284	2.280	39.9	3.383
		(4.20)	(0.89)	(133.8)	(46.1)		(88.7)	(2.286)	(2.287)	(99.3)	
II	81.95	4.14	1.03	128.8	60.4	10.0	87.0	2.270	2.275	40.1	3.359
		(4.22)	(0.99)	(132.1)	(51.9)		(85.0)	(2.337)	(2.275)	(98.1)	
III	89.83	4.15	1.30	117.9	68.7	12.0	84.1	2.522	2.265	40.0	3.351
		(4.90)	(0.95)	(140.3)	(43.1)		(85.3)	(2.643)	(2.286)	(41.0)	
IV	96.74	4.20	1.04	127.2	65.9	13.5	82.7	2.267	2.267	98.1	3.325
		(4.32)	(0.92)	(133.8)	(53.3)		(83.1)	(2.270)	(2.270)	(98.3)	

3.3 The π-Ligands Effect on the Electronic Geometries and Properties of Catalysts I-IV

Considering the size of the π-ligands in catalysts **I-IV**, the number of aromatic ring is in the order of **I** < **II** < **III** = **IV**. This increment in the size of the π-ligands within the catalysts was found to have a significant effect on the electronic geometries of the catalysts. We observed a decrease in the angle (δ) formed between the metal and the centroid changing from 87.5° (**I**) → 87.0° (**II**) → 84.1° (**III**) → 82.7° (**IV**). This is due to an increase in the van der Waals (VDW) interaction between the aromatic ring of the π-ligand and the methyl groups at the Zr atom. The lowest angle (δ) observed in catalyst **IV** is due to the VDW interaction between two methyl groups and two benzene rings of the fluoryl ligand. With the strong VDW in catalyst **IV**, the X-M-X angle was found to be two-fold large (~98°) compared to that for other catalysts (**I-III**) (~40°), as shown in Table 2. Among the four catalysts, catalyst **III** has the most steric hindrance between one methyl group of Zr atom and the two benzene rings of the indene ligands. That is why the highest value of both β and M-Cen was observed in catalyst **III**.

The π-ligand introduction has a significant effect on the electronic properties. We found a decrease in the HOMO-LUMO energy gap for the four catalysts in the order of **I** > **II** > **III** > **IV**, as shown in Figure 4, associated with the decreased dipole moment (Table 3). We also observed a positive charge on the Si and Zr in all catalysts, with Si carrying the most.

Table 3. Energy, frontier orbital (HOMO,LUMO), dipole moment and Muliken charges (*e*) of catalysts **I-IV**.

Catalyst	Energy (a.u.)	LUMO (eV)	HOMO (eV)	Δ(LUMO-HOMO)	Dipole moment	Mulliken charges (*e*) of Si/Zr
I	-596.040	-1.225	-6.177	4.95	2.01	1.228/0.765
II	-749.672	-1.197	-5.470	4.27	1.78	1.242/0.785
III	-903.303	-1.252	-5.306	4.05	1.62	1.252/0.788
IV	-903.306	-1.361	-5.170	3.81	1.47	1.239/0.805

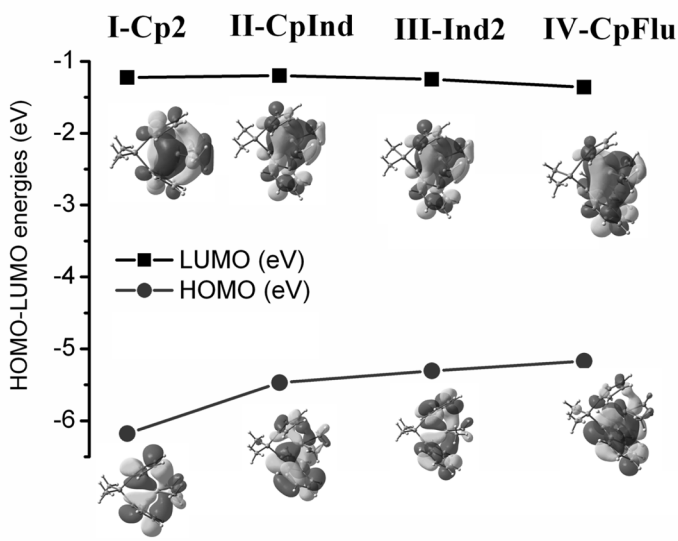

Figure 4. HOMO-LUMO energy gaps and frontier orbitals of catalysts **I-IV**.

3.4 Analysis of Regioselectivity of ε-CL from the Monomer-Inserted Complex Structure

To understand a regioselectivity for the monomer-insertion step of the ROP of ε-CL using those title catalysts (**I-IV**), the electronic structures of the monomer-inserted complex with different monomer insertions were analyzed. The optimized structures for the monomer complexes (**I-IV**) were calculated at the B3LYP/LANL2DZ level of theory and the results are illustrated in Figures 5-8. We found that the possible number of monomer-inserted complex depends on the symmetry of the catalyst. Two possible orientations of the monomer are observed for catalyst **I** and **IV** due to the C_{2v} symmetry, as shown in Figures 5 and 8. On the other hand, catalysts **II** and **III** with the C_1 symmetry gave four possible orientations of monomer. Excluding of catalyst **III**, the most energetically stable structure for each catalyst was found to share the same conformation with the ester group of the monomer pointing away from the methyl group at Zr atom (see complexes **I-a**, **II-a**, and **IV-a** in Figures 5, 6 and 8). The orientation of the catalysts was found to correspond well with the shortest distance of Zr-O1 bond (~2.18 Å- ~2.19 Å). In case of catalyst **III**, the most stable structure was found in complex **III-c** in which the ester group still keeps pointing to the catalyst but its monomer is situated at the other side, due to a steric influence from the π-ligand. A planar conformation in the lactone ring was also observed in all catalysts, with the C1-C2-O2-C3 torsion angle of -4.41° - 3.45°, suggesting that the geometric rearrangement is required for each insertion

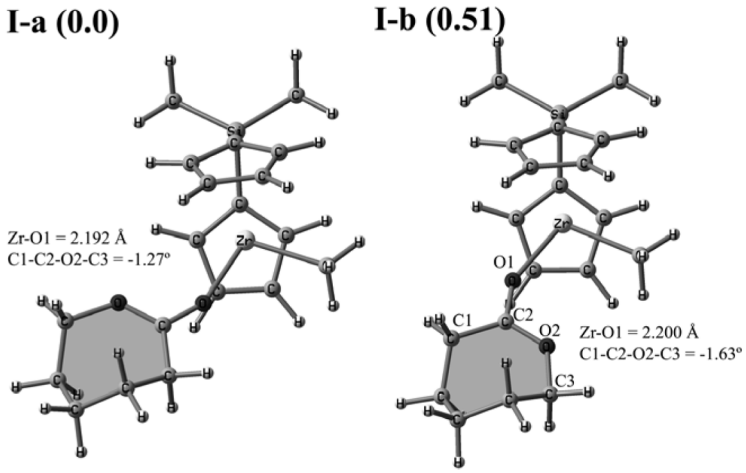

Figure 5. Activated complex structure of catalyst **I** with different ε-caprolactone insertions calculated at the B3LYP/LANL2DZ level of theory. Relative energies are indicated in parenthesis.

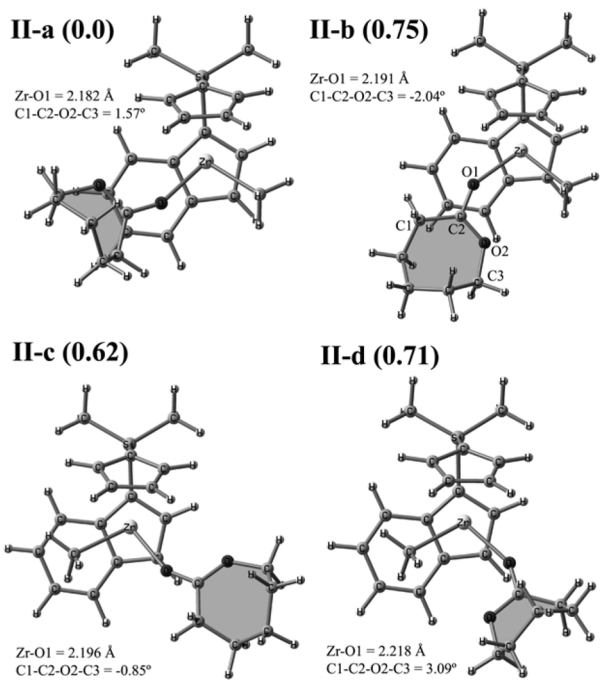

Figure 6. Activated complex structure of catalyst **II** with different ε-caprolactone insertions calculated at the B3LYP/LANL2DZ level of theory. Relative energies are indicated in parenthesis.

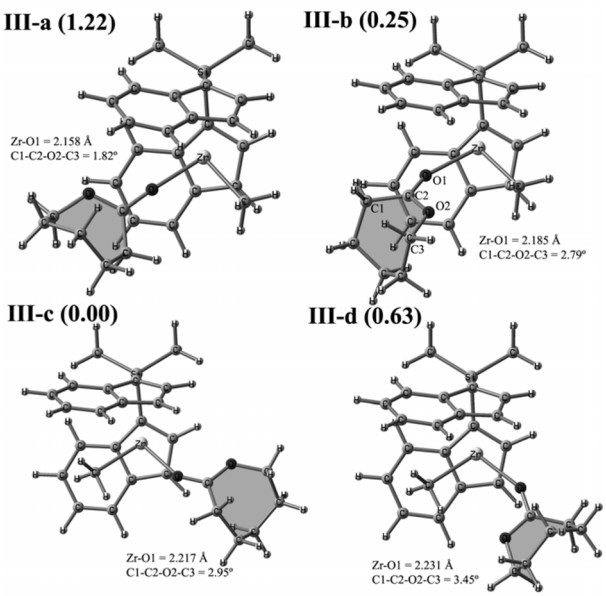

Figure 7. Activated complex structure of catalyst **III** with different ε-caprolactone insertions calculated at the B3LYP/LANL2DZ level of theory. Relative energies are indicated in parenthesis.

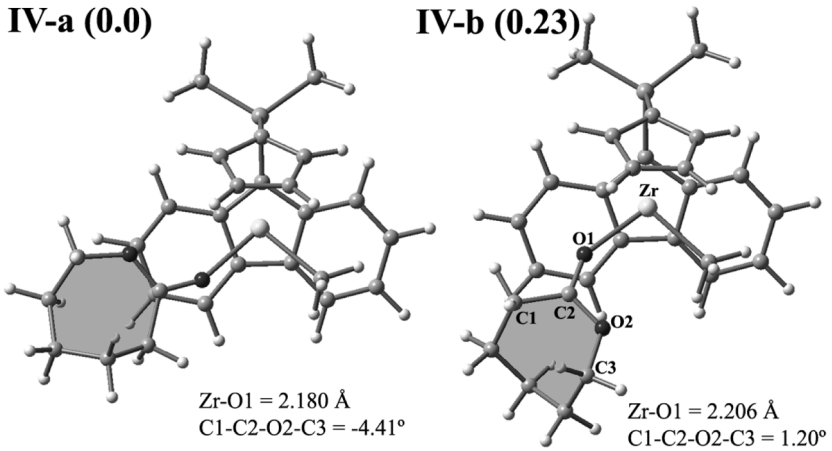

Figure 8. Activated complex structure of catalyst **IV** with different ε-caprolactone insertions calculated at the B3LYP/LANL2DZ level of theory. Relative energies are indicated in parenthesis.

4. CONCLUSIONS

In this paper, we present the computational analyses for the electronic structures and properties of four bridged dimethylzirconocene catalysts (**I-IV**) bearing different π-ligands such as cyclopentadienyl, indenyl or fluorenyl ligands. The introduction of the silicon-bridge and the π-ligands had a profound effect on the electronic geometries and properties in all four catalysts. In comparison with the unbridged catalysts, we observed a constrained geometry for all bridged catalyst with the Zr atom moving away from the catalyst center to some extent. The energy intervals between LUMO and HOMO and the dipole moments for the four catalysts are in the order of **I** > **II** > **III** > **IV**. The positive charges are observed only on Si and Zr for each of the four complexes. We then examined the monomer-inserted complexes of all catalysts and found that, excluding of catalyst **III**, most energetic favorable structures of the complexes have the shortest Zr-O distance with a stable conformation having the ester group of the monomer pointing to the catalyst. A steric hindrance is dominant in catalyst **III**, thus giving the different complex structure. In addition, a planar conformation in the lactone ring was also observed in all catalysts. These data provide a structural basis of dimethyl zirconocene and dimethyl zirconocene-monomer complex, which will be helpful for further experimental and theoretical investigations on the ROP of ε-CL initiated by group 4 metallocene catalyst.

ACKNOWLEDGEMENTS

This work is supported by grants from the University of Phayao (R020056216016) and the Thailand Research Fund (MRG-5680143). We thank Dr. Jon I. Mujika for helpful comments and Dr. Banjong Chairinkham for editorial assistance. J.J. would like to thank National e-Science Infrastructure Consortium for providing computing resources that have contributed to the research results reported within this paper (URL: http://www.e-science.in.th).

REFERENCES

[1] Seyednejad H., Ghassemi A.H., van Nostrum C.F., Vermonden T. and Hennink W.E., Functional aliphatic polyesters for biomedical and pharmaceutical applications, *J. Control Release*, 2011; **152**: 168-176.

[2] Khan J.H., Schue F. and George G.A., Heterogeneous ring-opening polymerization of lactones for biomedical applications, *Polym. Inter.*, 2009; **58**: 296-301.

[3] Albertsson A.C. and Varma I.K., Recent developments in ring opening polymerization of lactones for biomedical applications, *Biomacromolecules*, 2003; **4**: 1466-1486.

[4] Meelua W., Bua-Own V., Molloy R. and Punyodom W., Comparison of metal alkoxide initiators in the ring-opening polymerization of caprolactone, *Adv. Mater. Res.*, 2012; **506**: 142-145.

[5] Gao A., Mu Y., Zhang J. and Yao W., Aluminum complexes with bidentate N,N-dialkylaniline-arylamido ligands: synthesis, structures, and catalytic properties for efficient ring-opening polymerization of e-caprolactone, *Eur. J. Inorg. Chem.*, 2009; **2009**: 3613-3621.

[6] Dumklang M., Pattawong N., Punyodom W., Meepowpan P., Molloy R. and Hoffman M., Novel tin(II) butoxides for use as initiators in the ring-opening polymerisation of ε-caprolactone, *Chiang Mai J. Sci.*, 2009; **36**: 136-148.

[7] Huang B.H., Lin C.N., Hsueh M.L., Athar T. and Lin C.C., Well-defined sterically hindered zinc aryloxides: Excellent catalysts for ring-opening polymerization of [var epsilon]-caprolactone and l-lactide, *Polymer*, 2006; **47**: 6622-6629.

[8] Sheng H., Li J., Zhang Y., Yao Y. and Shen Q., $LnNa_8[OC(CH_3)_3]_{10}(OH)$ alkoxide clusters: Highly active single-component catalysts for the homopolymerization and copolymerization of ε-caprolactone and trimethylene carbonate, *J. Appl. Polym. Sci.*, 2009; **112**: 454-460.

[9] Meelua W., Molloy R., Meepowpan P. and Punyodom W., Isoconversional kinetic analysis of ring-opening polymerization of ε-caprolactone: Steric influence of titanium(IV) alkoxides as initiators, *J. Polym. Res.*, 2012; **19**: 9799-9810.

[10] Hayakawa M., Mitani M., Yamada T. and Mukaiyama T., Living ring-opening polymerization of lactones using cationic zirconocene complex catalysts, *Macromol. Chem. Phys.*, 1997; **198**: 1305-1317.

[11] Kostakis K., Mourmouris S., Karanikolopoulos G., Pitsikalis M. and Hadjichristidis N., Ring-opening polymerization of lactones using zirconocene catalytic systems: block copolymerization with methyl methacrylate, *J. Polym Sci. Part A: Polym. Chem.*, 2007; **45**: 3524-3537.

[12] Villaseñor E., Gutierrez-Gonzalez R., Carrillo-Hermosilla F., Fernández-Galán R., López-Solera I., Fernández-Pacheco A.R. and Antiñolo A., Neutral dimethylzirconocene complexes as initiators for the ring-opening polymerization of ε-caprolactone, *Eur. J. Inorg. Chem.*, 2013; **2013**: 1184-1196.

[13] Gaussian 09, Revision B.01, Gaussian Inc., Wallingford CT, USA, 2010.

[14] Yang Y., Weaver M.N. and Merz K.M., Jr., Assessment of the "6-31+G** + LANL2DZ" mixed basis set coupled with density functional theory methods and the effective core potential: Prediction of heats of formation and ionization potentials for first-row-transition-metal complexes, *J. Phys. Chem. A.*, 2009; **113**: 9843-9851.

[15] Cramer C.J. and Truhlar D.G., Density functional theory for transition metals and transition metal chemistry, *Phys. Chem. Chem. Phys.*, 2009; **11**: 10757-10816.